

Investigating nuclear dissipation properties at large deformations via excitation energy at scission

Jian Tian¹ · Wei Ye¹

Received: 15 August 2016/Revised: 15 August 2016/Accepted: 8 October 2016/Published online: 31 October 2016
© Shanghai Institute of Applied Physics, Chinese Academy of Sciences, Chinese Nuclear Society, Science Press China and Springer Science+Business Media Singapore 2016

Abstract Using the stochastic Langevin model coupled with a statistical decay model, we study nuclear dissipation properties at large deformations with excitation energy at scission (E_{sc}^*) measured in experiments. It is found that the postsaddle dissipation strength required to fit E_{sc}^* data is $12 \times 10^{21} \text{ s}^{-1}$ for $^{254,256}\text{Fm}$ and $6 \times 10^{21} \text{ s}^{-1}$ for ^{189}Au , which has a smaller postsaddle deformation than the former heavy nucleus, showing a rise of nuclear dissipation strength with increasing deformation.

Keywords Excitation energy at scission · Langevin model · Nuclear dissipation

1 Introduction

The precise nature of nuclear dissipation remains one of the major problems unresolved in nuclear physics. Dissipation plays a critical role in low-energy nucleus–nucleus collision dynamics [1–7]. It delays fission, resulting in an enhanced emission of prescission light particles and a large evaporation residue cross section with respect to the predictions of standard statistical models [8–10]. Accordingly, information on dissipation in fission is gained by comparing theory and experiment [11–14]. It has been shown [15–19] that dynamical Langevin models of fission

describe well a great number of experimental observables, including particle multiplicities and evaporation residue cross sections, for a great number of compound nuclei (CNs) over a broad range of excitation energy, angular momentum, and fissility.

Numerous theoretical investigations indicate that nuclear dissipation is shape dependent [11, 16, 20, 21], and the shape dependence of the nuclear dissipation is identified as a key ingredient [22] in the application of Langevin models to fission of excited nuclei. Currently, intensive efforts are being put on the strength of presaddle dissipation [23–25], and only very few studies focus on the exploration of postsaddle dissipation characteristics.

Light particles are considered to be the main indicators [20, 21, 26] for the dissipation effects. However, they can be evaporated along the whole fission path during the fission process of the CN, which causes an experimental difficulty of distinguishing particles emitted prior to saddle from those of the saddle-to-scission region.

Excitation energy at scission (E_{sc}^*) is observable and can be used to survey nuclear dissipation [27]. It not only is related to the number of prescission particles, but also depends on the energy loss taken away by these evaporated particles. Both aspects are connected with the properties of nuclear dissipation. So the quantity, E_{sc}^* , carries ample information on nuclear dissipation. As an independent information source, the E_{sc}^* thus constitutes an alternative tool of exploiting postsaddle dissipation properties.

Till now, few researchers have used experimental E_{sc}^* data to pin down postsaddle dissipation. In the present work, the E_{sc}^* data from heavy $^{254,256}\text{Fm}$ and light ^{189}Au systems will be employed to probe postsaddle nuclear dissipation.

This work was supported by the National Nature Science Foundation of China (No. 11575044).

✉ Wei Ye
yewei@seu.edu.cn

¹ Department of Physics, Southeast University, Nanjing 210096, China

2 Theoretical model

A brief account of the combination of the dynamical Langevin equation with a statistical decay model (CDSM) [20, 28] is given here. The dynamic part of CDSM is described by the Langevin equation that is expressed by entropy. We employ the following one-dimensional overdamped Langevin equation to perform the trajectory calculations.

$$\frac{dq}{dt} = \frac{T}{M\beta} \frac{dS}{dq} + \sqrt{\frac{T}{M\beta}} \Gamma(t). \tag{1}$$

Here, q is the dimensionless fission coordinate and defined as half of the distance between the center of mass of the future fission fragments divided by the radius of the compound nucleus. T is the temperature, and $\langle \Gamma(t) \rangle$ is a fluctuating force with $\langle \Gamma(t) \rangle = 0$. M is the inertia parameter [20], and β is the dissipation strength.

The driving force of the Langevin equation is calculated from entropy:

$$S(q, E^*) = 2\sqrt{a(q)[E^* - V(q)]}, \tag{2}$$

where E^* is the excitation energy of the system. Equation (2) is constructed from the Fermi gas expression with a finite-range liquid-drop potential [29]. The q -dependent surface, coulomb, and rotation energy terms are included in the potential $V(q)$.

In constructing the entropy, the following deformation-dependent level density parameter is used:

$$a(q) = a_1A + a_2A^{2/3}B_s(q), \tag{3}$$

where $a_1 = 0.073 \text{ MeV}^{-1}$ and $a_2 = 0.095 \text{ MeV}^{-1}$ are taken from Ignatyuk et al. [30]. B_s is the dimensionless surface area (for sphere $B_s = 1$), which can be parametrized by the analytical expression [31],

$$B_s(q) = \begin{cases} 1 + 2.844(q - 0.375)^2, & \text{if } q < 0.452 \\ 0.983 + 0.439(q - 0.375), & \text{if } q \geq 0.452. \end{cases} \tag{4}$$

In the CDSM, light-particle evaporation is coupled to the fission mode by a Monte Carlo procedure [16]. The emission width of a particle of kind v is given by Ref. [32].

$$\Gamma_v = (2s_v + 1) \frac{m_v}{\pi^2 \hbar^2 \rho_c(E^*)} \times \int_0^{E^* - B_v} d\varepsilon_v \rho_R(E^* - B_v - \varepsilon_v) \varepsilon_v \sigma_{\text{inv}}(\varepsilon_v), \tag{5}$$

where s_v is the spin of the emitted particle v , and m_v is its reduced mass with respect to the residual nucleus. The level densities of the compound and residual nuclei are denoted by $\rho_c(E^*)$ and $\rho_R(E^* - B_v - \varepsilon_v)$. B_v are the liquid-

drop binding energies. ε is the kinetic energy of the emitted particle, and $\sigma_{\text{inv}}(\varepsilon_v)$ is the inverse cross sections [32].

After each emission act of a particle, the intrinsic energy, entropy, and temperature in the Langevin equation are recalculated and the dynamics are continued. Precision various particle multiplicities are calculated by counting the number of corresponding evaporated particle events registered in the CDSM. To accumulate sufficient statistics, 10^7 Langevin trajectories are simulated.

Regarding the excitation energy at scission, it is determined by using energy conservation law,

$$E^* = E_{\text{sc}}^* + E_{\text{coll}} + V(q) + E_{\text{evap}}(t_{\text{sc}}), \tag{6}$$

where E^* and $V(q)$ have the same meaning mentioned earlier. E_{coll} is the kinetic energy of the collective degrees of freedom [20], and $E_{\text{evap}}(t_{\text{sc}})$ is the energy carried away by all evaporated particles by the scission time, t_{sc} .

For starting a trajectory, an orbit angular momentum value is sampled from the fusion spin distribution, which reads:

$$\frac{d\sigma(\ell)}{d\ell} = \frac{2\pi}{k^2} \frac{2\ell + 1}{1 + \exp[(\ell - \ell_c)/\delta\ell]}. \tag{7}$$

The parameters ℓ_c and $\delta\ell$ are the critical angular momenta for fusion and diffuseness, respectively.

3 Results and discussion

During the decay process of a CN, particle evaporation channel competes with fission channel. The nuclear friction retards fission and enhances particle emission, which lowers the excitation energy at scission.

To better explore postsaddle dissipation properties with E_{sc}^* in this work, the presaddle friction strength is set to 3 zs^{-1} ($1 \text{ zs} = 10^{-21} \text{ s}$), in agreement with recent theoretical estimates and experimental analyses [12, 21, 28, 33–35]. The postsaddle friction strength (β) is determined by reproducing measured E_{sc}^* in $^{16}\text{O} + ^{238}\text{U}$ [36], $^{18}\text{O} + ^{238}\text{U}$ [36], and $^{20}\text{Ne} + ^{169}\text{Tm}$ [37] reactions.

Figure 1a displays a comparison between experimental E_{sc}^* data of the ^{254}Fm system and theoretical ones which are calculated with Langevin models. It shows that E_{sc}^* is a decreasing function of β . The reason for this behavior is that dissipation hinders fission, increasing particle emission and hence yielding a small excitation energy at scission. A detailed comparison of model calculations with experimental data reveals that the best-fit value of β is 12.5 zs^{-1} (represented by solid square).

We also analyze the E_{sc}^* data from another heavy ^{256}Fm nucleus, produced in $^{18}\text{O} + ^{238}\text{U}$ reaction, and observe from Fig. 1b that the best-fit friction strength is $\sim 11.5 \text{ zs}^{-1}$, an amplitude analogous to that of ^{254}Fm .

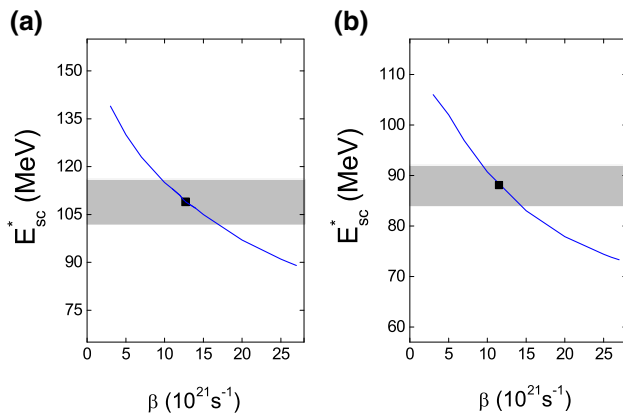


Fig. 1 (Color online) Theoretical calculations are compared with measured excitation energy at scission for **a** ^{16}O ($E_{\text{lab}} = 288$ MeV) + $^{238}\text{U} \rightarrow ^{254}\text{Fm}$ and **b** ^{18}O ($E_{\text{lab}} = 159$ MeV) + $^{238}\text{U} \rightarrow ^{256}\text{Fm}$ reactions. Experimental values [36] are represented by the shaded band. Solid lines are predictions from Langevin models

Overall, the postsaddle friction strength deduced from the two heavy systems (~ 12 zs^{-1}) is stronger than that of presaddle friction, demonstrating a rise of the friction strength with increasing deformation.

A CN undergoes deformation as it fissions. As is well known, a light CN system has a shorter saddle-to-scission distance than a heavy one. It means that the E_{sc}^* data from light and heavy fissioning systems can be employed to probe the friction strength at different deformations. To that end, we choose a light ^{189}Au system produced in $^{20}\text{Ne} + ^{169}\text{Tm}$. The comparison between experimental data and calculated results is presented in Fig. 2. It is clear that E_{sc}^* gets larger with the increase in incident energy as a result

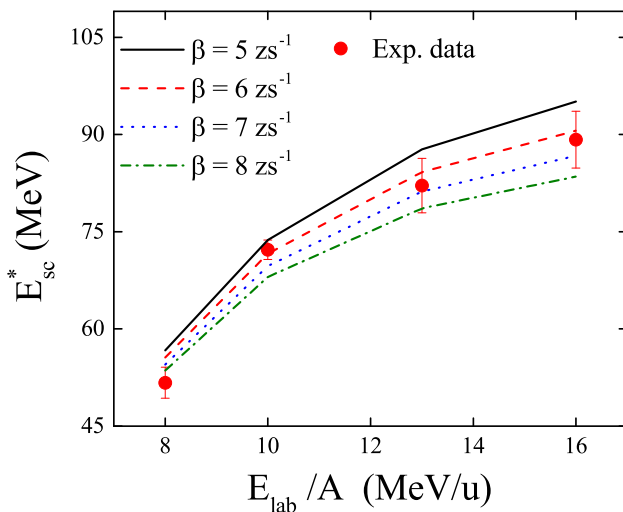


Fig. 2 (Color online) Calculated and experimental excitation energy at scission in the system $^{20}\text{Ne} + ^{169}\text{Tm} \rightarrow ^{189}\text{Au}$ at different laboratory energy per nucleon [37]. Curves represent model calculations at postsaddle friction strengths $\beta = 5, 6, 7,$ and 8 zs^{-1}

of a high initial excitation energy. In addition, a greater β leads to a smaller E_{sc}^* , because more particles are evaporated at a larger friction, which significantly reduces the excitation energy at scission. By comparing the experimental and calculated E_{sc}^* , one can notice that the friction strength of ~ 6 zs^{-1} can provide a satisfactory description of the experimental data. This friction strength is slightly stronger than that of the presaddle region, a result that is consistent with that derived from the heavy Fm systems.

It has been noted [21] that, when a modified one-body dissipation strength (which assumes a decreasing function of friction with deformation) was used in the calculation, the theoretical predictions are far below precision particle multiplicity data of heavy fissioning nuclei with $A > 250$. For these very heavy nuclei, there is a longer distance between the saddle point and scission and hence a larger deformation is involved. It means that to account for the multiplicity data from heavy decaying systems, it is necessary to introduce a strong postsaddle friction in model calculations.

In addition to E_{sc}^* , we further survey particle multiplicity from light and heavy fissioning systems. As an illustration, Fig. 3 shows the comparison between theoretical and experimental precision neutrons for ^{256}Fm and ^{189}Au . The best-fit postsaddle friction value required to fit data is found to be 11 zs^{-1} for heavy ^{256}Fm and 5.5 zs^{-1} for light ^{189}Au . While the result that a stronger postsaddle friction at a larger deformation is not altered, these best-fit β values obtained from precision neutron data are slightly different from those obtained from the E_{sc}^* data. This could be due to a consequence of a difference in the sensitivity that different observables to friction.

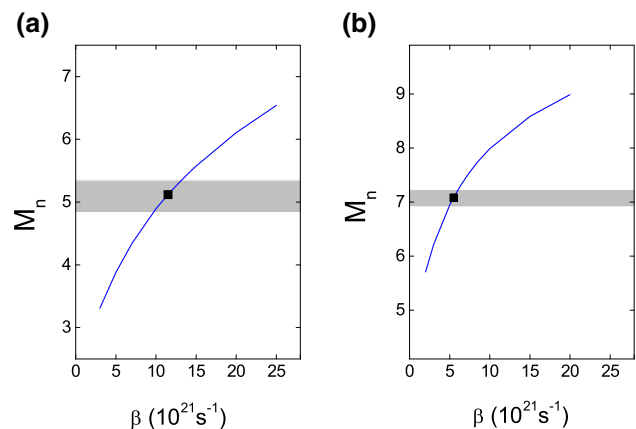


Fig. 3 (Color online) Comparison of Langevin predictions for precision neutrons with measured values in **a** ^{18}O ($E_{\text{lab}} = 159$ MeV) + $^{238}\text{U} \rightarrow ^{256}\text{Fm}$ and **b** ^{20}Ne ($E_{\text{lab}} = 320$ MeV) + $^{169}\text{Tm} \rightarrow ^{189}\text{Au}$ reactions. Experimental values [36, 37] are shown by the shaded band, and model calculations are displayed by solid lines

4 Summary

In the framework of Langevin model of fission dynamics, we have compared calculated and measured excitation energy at scission from heavy and light fissioning systems. A postsaddle friction value of $12 \times 10^{21} \text{ s}^{-1}$ and $6 \times 10^{21} \text{ s}^{-1}$ is extracted for $^{248,256}\text{Fm}$ and ^{189}Au nuclei, respectively. Postsaddle deformation of ^{189}Au is smaller than that of $^{248,256}\text{Fm}$, and thus an evident difference in the deduced friction strength for the light and heavy nuclei shows that nuclear friction becomes strong with an increase in deformation.

References

- D. Hilscher, H. Rossner, *Ann. Phys.* **17**, 471 (1992). doi:[10.1051/anphys:01992001706047100](https://doi.org/10.1051/anphys:01992001706047100)
- J.U. Andersen, J. Chevallier, J.S. Forster et al., Attosecond time delays in heavy-ion induced fission measured by crystal blocking. *Phys. Rev. C* **78**, 064609 (2008). doi:[10.1103/PhysRevC.78.064609](https://doi.org/10.1103/PhysRevC.78.064609)
- W.Q. Shen, J. Albinski, A. Gobbi et al., Fission and quasifission in U-induced reactions. *Phys. Rev. C* **36**, 115 (1987). doi:[10.1103/PhysRevC.36.115](https://doi.org/10.1103/PhysRevC.36.115)
- J. Velkovska, C.R. Morton, R.L. McGrath et al., Quasifission reactions as a probe of nuclear viscosity. *Phys. Rev. C* **59**, 1506 (1999). doi:[10.1103/PhysRevC.59.1506](https://doi.org/10.1103/PhysRevC.59.1506)
- E. Williams, D.J. Hinde, M. Dasgupta et al., Evolution of signatures of quasifission in reactions forming curium. *Phys. Rev. C* **88**, 034611 (2013). doi:[10.1103/PhysRevC.88.034611](https://doi.org/10.1103/PhysRevC.88.034611)
- A.K. Nasirov, G. Giardina, G. Mandaglio et al., Quasifission and fusion-fission in reactions with massive nuclei: comparison of reactions leading to the $Z = 120$ element. *Phys. Rev. C* **79**, 024606 (2009). doi:[10.1103/PhysRevC.79.024606](https://doi.org/10.1103/PhysRevC.79.024606)
- Y. Aritomo, Fusion hindrance and roles of shell effects in superheavy mass region. *Nucl. Phys. A* **88**, 034611 (2013). doi:[10.1016/j.nuclphysa.2006.09.018](https://doi.org/10.1016/j.nuclphysa.2006.09.018)
- J. Benlliure, E. Casarejos, J. Pereira et al., Transient and quasi-stationary dissipative effects in the fission flux across the barrier in $1\text{A GeV }^{238}\text{U}$ on deuterium reactions. *Phys. Rev. C* **74**, 014609 (2006). doi:[10.1103/PhysRevC.74.014609](https://doi.org/10.1103/PhysRevC.74.014609)
- H. Singh, K.S. Golda, Santanu Pal et al., Role of nuclear dissipation and entrance channel mass asymmetry in pre-scission neutron multiplicity enhancement in fusion-fission reactions. *Phys. Rev. C* **78**, 024609 (2008). doi:[10.1103/PhysRevC.78.024609](https://doi.org/10.1103/PhysRevC.78.024609)
- R. Sandal, B.R. Behera, V. Singh et al., Effect of N/Z in pre-scission neutron multiplicity for $^{16,18}\text{O} + ^{194,198}\text{Pt}$ systems. *Phys. Rev. C* **87**, 014604 (2013). doi:[10.1103/PhysRevC.87.014604](https://doi.org/10.1103/PhysRevC.87.014604)
- J. Sadhukhan, S. Pal, Critical comparison of Kramers' fission width with the stationary width from the Langevin equation. *Phys. Rev. C* **79**, 064606 (2009). doi:[10.1103/PhysRevC.79.064606](https://doi.org/10.1103/PhysRevC.79.064606)
- W. Ye, Heavy-ion versus $^3\text{He}/^4\text{He}$ fusion-fission reactions: Angular momentum dependence of dissipation in nuclear fission. *Phys. Rev. C* **84**, 034617 (2011). doi:[10.1103/PhysRevC.84.034617](https://doi.org/10.1103/PhysRevC.84.034617)
- V. Singh, B.R. Behera, Maninder Kaur et al., Neutron multiplicity measurements for $^{19}\text{F} + ^{194,196,198}\text{Pt}$ systems to investigate the effect of shell closure on nuclear dissipation. *Phys. Rev. C* **87**, 064601 (2013). doi:[10.1103/PhysRevC.87.064601](https://doi.org/10.1103/PhysRevC.87.064601)
- Y. Ayyad, J. Benlliure, E. Casarejos et al., Proton-induced fission of ^{181}Ta at high excitation energies. *Phys. Rev. C* **89**, 054610 (2014). doi:[10.1103/PhysRevC.89.054610](https://doi.org/10.1103/PhysRevC.89.054610)
- P. Fröbrich, I.I. Gontchar, Langevin fluctuation-dissipation dynamics of hot nuclei: pre-scission neutron multiplicities and fission probabilities. *Nucl. Phys. A* **556**, 281 (1993). doi:[10.1016/0375-9474\(93\)90352-X](https://doi.org/10.1016/0375-9474(93)90352-X)
- K. Pomorski, B. Nerlo-Pomorskaa, A. Surowieca et al., Light-particle emission from the fissioning nuclei ^{126}Ba , ^{188}Pt and $^{266,272,278}110$: theoretical predictions and experimental results. *Nucl. Phys. A* **679**, 25 (2000). doi:[10.1016/S0375-9474\(00\)00327-4](https://doi.org/10.1016/S0375-9474(00)00327-4)
- W. Ye, Role of N/Z in giant dipole resonance γ rays as a probe of post-saddle nuclear dissipation. *Phys. Lett. B* **681**, 413 (2000). doi:[10.1016/j.physletb.2009.10.067](https://doi.org/10.1016/j.physletb.2009.10.067)
- A.V. Karpov, P.N. Nadtochy, D.V. Vanin et al., Three-dimensional Langevin calculations of fission fragment mass-energy distribution from excited compound nuclei. *Phys. Rev. C* **63**, 054610 (2001). doi:[10.1103/PhysRevC.63.054610](https://doi.org/10.1103/PhysRevC.63.054610)
- Jhilam Sadhukhan, Santanu Pal, Role of saddle-to-scission dynamics in fission fragment mass distribution. *Phys. Rev. C* **84**, 044610 (2011). doi:[10.1103/PhysRevC.84.044610](https://doi.org/10.1103/PhysRevC.84.044610)
- P. Fröbrich, I.I. Gontchar, Langevin description of fusion, deep-inelastic collisions and heavy-ion-induced fission. *Phys. Rep.* **292**, 131 (1998). doi:[10.1016/S0370-1573\(97\)00042-2](https://doi.org/10.1016/S0370-1573(97)00042-2)
- P.N. Nadtochy, G.D. Adeev, A.V. Karpov, More detailed study of fission dynamics in fusion-fission reactions within a stochastic approach. *Phys. Rev. C* **65**, 064615 (2002). doi:[10.1103/PhysRevC.65.064615](https://doi.org/10.1103/PhysRevC.65.064615)
- H.J. Krappe, K. Pomorski, *Theory of Nuclear Fission*. Lecture Notes in Physics Vol. 838 (Springer, Berlin, 2012)
- W. Ye, N. Wang, Significant role of level-density parameters in probing nuclear dissipation with light-ion-induced fission excitation functions. *Phys. Rev. C* **87**, 014610 (2013). doi:[10.1103/PhysRevC.87.014610](https://doi.org/10.1103/PhysRevC.87.014610)
- B.B. Back, D.J. Blumenthal, C.N. Davids et al., Fission hindrance in hot ^{216}Th : evaporation residue measurements. *Phys. Rev. C* **74**, 044602 (1999). doi:[10.1103/PhysRevC.74.044602](https://doi.org/10.1103/PhysRevC.74.044602)
- P.D. Shidling, N.M. Badiger, S. Nath et al., Fission hindrance studies in ^{200}Pb : evaporation residue cross section and spin distribution measurements. *Phys. Rev. C* **60**, 064603 (1999). doi:[10.1103/PhysRevC.60.064603](https://doi.org/10.1103/PhysRevC.60.064603)
- K. Ramachandran, A. Chatterjee, A. Navin et al., Fission time scale from pre-scission neutron, proton, and α particle multiplicities in $^{28}\text{Si} + ^{175}\text{Lu}$. *Phys. Rev. C* **73**, 064609 (1999). doi:[10.1103/PhysRevC.73.064609](https://doi.org/10.1103/PhysRevC.73.064609)
- W. Ye, N. Wang, Spallation reaction and the probe of nuclear dissipation with excitation energy at scission. *Nucl. Sci. Tech.* **24**, 050521 (2013)
- P. Fröbrich, On the dynamics of fission of hot nuclei. *Nucl. Phys. A* **787**, 170 (2007). doi:[10.1016/j.nuclphysa.2006.12.028](https://doi.org/10.1016/j.nuclphysa.2006.12.028)
- P. Möller, W.D. Myers, W.J. Swiatecki et al., Nuclear mass formula with a finite-range droplet model and a folded-Yukawa single-particle potential. *At. Data Nucl. Data Tables* **39**, 225 (1988). doi:[10.1016/0092-640X\(88\)90023-X](https://doi.org/10.1016/0092-640X(88)90023-X)
- A.V. Ignatyuk, M.G. Itkis, V.N. Okolovich et al., Fission of pre-actinide nuclei. Excitation functions for the (α, f) reaction. *Yad. Fiz.* **21**, 1185 (1975)
- I.I. Gontchar, P. Fröbrich, Consistent dynamical and statistical description of fission of hot nuclei. *Phys. Rev. C* **47**, 2228 (1999). doi:[10.1103/PhysRevC.47.2228](https://doi.org/10.1103/PhysRevC.47.2228)
- M. Blann, Decay of deformed and superdeformed nuclei formed in heavy ion reactions. *Phys. Rev. C* **21**, 1770 (1980). doi:[10.1103/PhysRevC.21.1770](https://doi.org/10.1103/PhysRevC.21.1770)

33. C. Schmitt, P.N. Nadtochy, A. Heinz et al., First experiment on fission transients in highly fissile spherical nuclei produced by fragmentation of radioactive beams. *Phys. Rev. Lett* **99**, 042701 (2007). doi:[10.1103/PhysRevLett.99.042701](https://doi.org/10.1103/PhysRevLett.99.042701)
34. W. Ye, H.W. Yang, F. Wu, Isospin effects on the evaporation residue spin distribution. *Phys. Rev. C* **77**, 011302(R) (2008). doi:[10.1103/PhysRevC.77.011302](https://doi.org/10.1103/PhysRevC.77.011302)
35. B. Jurado, C. Schmitt, K.-H. Schmidt et al., Transient effects in fission from new experimental signatures. *Phys. Rev. Lett* **93**, 072501 (2004). doi:[10.1103/PhysRevLett.93.072501](https://doi.org/10.1103/PhysRevLett.93.072501)
36. D.J. Hinde, Neutron emission as a probe of fusion-fission and quasifission dynamics. *Phys. Rev. C* **45**, 1229 (1992). doi:[10.1103/PhysRevC.45.1229](https://doi.org/10.1103/PhysRevC.45.1229)
37. J. Cabrera, Th Keutgen, Y. El Masri et al., Fusion-fission and fusion-evaporation processes in $^{20}\text{Ne}+^{159}\text{Tb}$ and $^{20}\text{Ne}+^{169}\text{Tm}$ interactions between $E/A=8$ and 16 MeV. *Phys. Rev. C* **68**, 034613 (2003). doi:[10.1103/PhysRevC.68.034613](https://doi.org/10.1103/PhysRevC.68.034613)